Na Channels and Two Types of Ca Channels in Rat Pancreatic B Cells Identified with the Reverse Hemolytic Plaque Assay

M. HIRIART and D. R. MATTESON

From the Department of Biophysics, University of Maryland School of Medicine, Baltimore, Maryland 21201, and The Marine Biological Laboratory, Woods Hole, Massachusetts 02543

ABSTRACT The reverse hemolytic plaque assay (RHPA) was used to study the secretory properties of single rat pancreatic B cells, and to identify insulin-secreting cells for patch-clamp experiments. In secretion studies using the RHPA, we find that the percentage of secreting B cells and the amount of insulin secreted per B cell increase as the glucose concentration is raised from 0 to 20 mM. Using the whole-cell variation of the patch-clamp technique, we find that identified B cells have three types of channels capable of carrying inward current: (*a*) tetrodotoxin-sensitive, voltage-dependent Na channels, which are nearly completely inactivated at −40 mV, (*b*) fast deactivating (FD) Ca channels, and (*c*) slowly deactivating (SD) Ca channels. We have shown that Na channels are functionally significant to the B cell, because tetrodotoxin partially inhibits glucose-induced insulin secretion. The properties of FD and SD Ca channels differ in several respects. FD channels deactivate at −80 mV, with a time constant of 129 μs, they are half-maximally activated near +15 mV, they do not inactivate during 100 ms, they conduct Ba^{2+} better than Ca^{2+}, and they are very sensitive to washout during intracellular dialysis. SD channels, on the other hand, deactivate with a time constant of 2.8 ms, they are half-maximally activated near −5 mV, they inactivate rapidly, they conduct Ba^{2+} and Ca^{2+} equally well, and they are insensitive to washout.

INTRODUCTION

The pancreatic B cell was the first type of endocrine cell that was shown to be electrically excitable. The electrical activity in B cells consists of oscillations in the membrane potential between a relatively negative quiet phase and a depolarized plateau phase containing a train of small-amplitude spikes (Dean and Matthews, 1968, 1970; Meissner, 1976). Glucose, which stimulates the B cell to secrete insulin,

Address reprint requests to Dr. Donald Matteson, Dept. of Biophysics, University of Maryland, 660 W. Redwood St., Baltimore, MD 21201. Dr. Hiriart's present address is Centro de Investigacion y Estudios Avanzados, Instituto Politecnico Nacional, Departamento de Fisiologia, Biofisica y Neurociencias, AP 14-740, Mexico D.F., 07000, Mexico.

J. GEN. PHYSIOL. © The Rockefeller University Press · 0022-1295/88/05/0617/23 $2.00
Volume 91 May 1988 617–639

induces electrical activity, and, as the extracellular glucose concentration is raised, there is an increase in the percentage of time the B cell is depolarized and spiking (Meissner and Schmelz, 1974; Dean et al., 1975; Meissner and Atwater, 1976). Since the spikes are thought to be generated by voltage-dependent Ca channels (Ribalet and Beigelman, 1980), this had led naturally to the suggestion that electrical activity and secretion are related: glucose stimulates secretion by increasing the activation of Ca channels, which results in raised intracellular Ca and activation of exocytosis.

While this is an attractive hypothesis, it was not possible until recently to measure directly the activity of the channels responsible for B cell electrical activity. With the development of the patch-clamp technique (Hamill et al., 1981), the characterization of ionic channels in B cells has begun. The whole-cell variation of the patch-clamp technique has been used to characterize voltage-dependent Ca and K channels in pancreatic B cells isolated from neonatal rats (Satin and Cook, 1985), NMRI mice (Rorsman and Trube, 1986), and two clonal B cell lines (Findlay and Dunne, 1985; Matteson and Matschinsky, 1986; Rorsman et al., 1986). In normal, adult B cells, inward currents were reported to be carried mainly by a single population of Ca channels. A small percentage of the cells were found to have Na channels, but in one study these were thought to be α_1 or α_2 cells (Rorsman and Trube, 1986). A voltage-independent K channel that is inhibited by extracellular glucose is thought to be at least partially responsible for the initiation of electrical activity in B cells (Ashcroft et al., 1984; Misler et al., 1986).

We have used a technique that allows us to study secretion from single isolated B cells, and also to unambiguously identify B cells for patch-clamp experiments. The procedure utilizes the reverse hemolytic plaque assay (RHPA), which allows one to identify a cell on the basis of the hormone it secretes (Neill and Frawley, 1983). The RHPA makes use of the ability of antigen-antibody complexes to activate complement-induced lysis of sheep red blood cells (SRBC). In the assay, endocrine cells are plated on a lawn of SRBC that have insulin antibodies bound to their surface. Insulin secreted by a B cell binds to the antibody-coated SRBC in the vicinity of the B cell, and these SRBC are subsequently lysed by complement. The lysed SRBC form a visible "plaque" surrounding the B cell. Previously, the RHPA has been used with B cells to study the effect of cell coupling on insulin secretion (Salomon and Meda, 1986).

In our study, the RHPA was used to characterize glucose-dependent insulin secretion, and to study the effect of channel blockers on B cell secretory activity. The RHPA was also used to identify cells for patch-clamp experiments, so that we could be certain of recording from B cells capable of stimulus-secretion coupling. In the latter experiments, we found that nearly all identified rat B cells had Na channels and two types of Ca channels. The two Ca channel types are similar in many respects to the fast deactivating (FD) and slowly deactivating (SD) channels found in anterior pituitary cells (Armstrong and Matteson, 1985; Matteson and Armstrong, 1986; Cota, 1986). We speculate that SD channels, with their more negative activation threshold, might be responsible for initiating the plateau deplorization and that FD channels generate the spikes. A preliminary account of some of our results has been reported (Hiriart and Matteson, 1987).

METHODS

Dissociation and Culturing of B Cells

Pancreatic islet cells were isolated from 250–300-g male Sprague-Dawley rats. A three-step procedure was followed to obtain the cells: (*a*) collagenase digestion of the pancreas and hand-picking of the islets (Lacy and Kostianovsky, 1967), (*b*) dissociation of the cells (Meda et al., 1980), and (*c*) culturing of the isolated cells. Unless otherwise specified, all solutions used to isolate the cells and in the RHPA were supplemented with 1 mg/ml bovine serum albumin (BSA), 400 U/ml penicillin, and 200 μg/ml streptomycin. The acinar tissue was disrupted by injecting 5 ml of Hanks' containing 10 μg/ml gentamicin sulfate into the common bile duct. The pancreas was removed, placed in Hanks' containing collagenase (2.5 mg/ml), and gently agitated at 37°C until well digested (~30 min). The digested tissue was washed five times with ice-cold Hanks'. Islets were hand-picked with a Lang-Levi pipette two or three times to separate them from the acinar tissue. The isolated islets were washed twice in divalent-free Spinner salt solution (SSS) and incubated for 20 min in SSS with 5 mg/ml BSA and 15 mM glucose at 37°C. The islet cells were then dispersed by mechanical pipetting with a Pasteur pipette. The cell suspension was washed once with SSS and twice with RPMI 1640 medium, pelleting the cells between washes by centrifugation at 180 g for 10 min. The cells were suspended in RPMI 1640, plated on Falcon (Oxnard, CA) Primaria culture dishes, and incubated at 37°C in a humidified CO_2 incubator for 30 min to enhance the attachment of the cells. The complete culture medium was then added. It contained RPMI 1640, 10% fetal bovine serum, 2% glutamine, 16 mM glucose, 0.1 mM 3-isobutyl-1-methylxanthine (IBMX), 400 U/ml penicillin, and 200 μg/ml streptomycin. The cells were maintained in culture for up to 1 wk.

Reverse Hemolytic Plaque Assay

B cells were identified, and their secretion was studied, using the reverse hemolytic plaque assay (RHPA) developed by Neill and Frawley (1983) for secretion studies in pituitary cells. Salomon and Meda (1986) have used this assay to study contact-dependent regulation of hormone secretion in B cells.

SRBC were coupled to staphylococcal protein A (SPA) using chromium chloride. After the SRBC were washed three times with normal saline, 1 ml of packed SRBC was resuspended in 5 ml of saline to which 1 ml SPA (1 mg/ml) and 5 ml of a solution of chromium chloride (0.2 mg/ml in normal saline) were added. The mixture was incubated for 1 h at 30°C. The SRBC were washed twice with normal saline and once with RPMI 1640 and kept at 4°C for up to 1 wk as a 2% suspension in RPMI 1640.

Before starting the RHPA, islet cells that had been maintained in culture were harvested by incubating with 0.25 mg/ml trypsin in SSS at 37°C for 10 min, followed by mechanical trituration with a Pasteur pipette. The cells were then washed once with culture medium and twice with RPMI 1640 and suspended to the required concentration (~1 million cells/ml). The SPA-coated SRBC were washed three times and used as an 18% suspension.

The RHPA was performed in Cunningham chambers (cf. Smith et al., 1986) coated with poly-L-lysine hydrobromide (0.5 mg/ml). Equal volumes of islet cells and 18% SRBC suspensions were mixed, introduced into the Cunningham chambers, and incubated for 45 min at 37°C in a CO_2 incubator. After the cells attached, the chambers were flushed with the test solution containing insulin antiserum diluted 1:40 and incubated for 1–2 h. The test solution contained (millimolar): 137 NaCl, 5.4 KCl, 1.3 $CaCl_2$, 1.0 $MgSO_4$, 0.65 NaH_2PO_4, 0.43 KH_2PO_4, 10 HEPES, and 0–20 mM glucose. The chambers were then rinsed and incubated with guinea pig complement diluted 1:40 in RPMI 1640 for 30 min. At the end of

the incubations, the cells in the chambers were fixed with glutaraldehyde (4%) in normal saline, stained with toluidine blue, and analzyed.

When identified B cells were to be used for the patch-clamp experiments, the RHPA was performed on glass coverslips. After the assay was completed, the complement was removed and the coverslips were kept in complete culture medium for up to 1 wk.

Source of Reagents for RHPA and Culturing

Reagents were obtained from the following sources: collagenase type IV was from CooperBiochemical Products, Freehold, NJ; insulin antiserum was from Cambridge Medical Diagnostics, Billerica, MA; trypsin, 1:250, was from Difco, Detroit, MI; RPMI 1640, Hanks' balanced salt solution, fetal bovine serum, guinea pig complement, penicillin-streptomycin solution, and gentamicin were from Gibco, Grand Island, NY; BSA, fraction V, chromium chloride, staphylococcal protein A, poly-L-lysine hydrobromide (>380,000 mol wt), Spinner salts Eagle, glutaraldehyde, IBMX, and D-glucose were from Sigma Chemical Co., St. Louis, MO.

Secretion Measurements with the RHPA

To have a measure of the insulin secreted by individual B cells, we counted the percentage of endocrine cells that formed plaques in the RHPA, and we also measured the average plaque area from plaque-forming cells. We frequently encountered both single cells and small clumps of cells that formed plaques, but we only counted single cells for this analysis. When measuring the percentage of plaque-forming cells, we counted ~100 cells in each chamber. To measure the plaque area, we used a video camera attached to an Axiophot microscope (Carl Zeiss, Inc., New York, NY) to project an image of the plaque at a final magnification of 900 or 1,800×. The plaque diameter was measured by hand and the area was then calculated. Approximately 25 plaque areas were measured in each chamber. For all RHPA experiments, each experimental condition was performed in duplicate.

Patch-Clamp Recording

Our application of the whole-cell variation of the patch-clamp technique is essentially as previously described (Matteson and Armstrong, 1984, 1986). The volume of the experimental chamber was small (0.2–0.3 ml) to allow rapid solution changes. Solution was fed by gravity into the chamber and removed by suction. The end of the suction tube was beveled at a 45° angle, and the opening was covered with gold mesh (Ted Pella, Tustin, CA) to minimize mechanical disturbances. The chamber volume was controlled by adjusting the height of the suction tube. B cells were plated into slivers of coverslips that were sized to fit this chamber. Low-resistance (1–2 MΩ) patch electrodes were pulled from soda-lime, Corning 8161, or Kimax glass (Kimble Glass Co., Vineland, NJ). A low access resistance between the pipette and the cell interior was required to faithfully record the fast component of Ca tail current that is reported here. Capacity transient cancellation was accomplished by feeding two or three exponential components to the ballistic charging capacitor connected to the negative input of the head-stage current-voltage converter. Series resistance compensation was used to compensate for some of the access resistance. Pulse generation and data acquisition were controlled by a PDP 11/23 computer (Digital Equipment Corp., Marlboro, MA). The holding potential was −80 mV in all voltage-clamp experiments. The linear components of current were subtracted by the computer with a P/2 procedure using control pulses from −120 mV (Armstrong and Benzanilla, 1974).

Solutions

The ionic compositions of the solutions used in these experiments are shown in Table I. Outward currents were eliminated by using Cs rather than K in internal solutions. When

measuring Na currents, 30 mM Na was present in the internal solution to allow us to measure the outward Na current. Although not specified in Table I, when measuring Ca currents, 3–5 mM MgATP was included in the internal solution to decrease the rate of Ca channel rundown.

Separation of Tail Current Components

Much of our analysis of Ca currents involved estimation of the amplitude of fast and slow tail current components. This was done by fitting tail currents with the sum of two exponentials as described in Matteson and Armstrong (1986). Basically, this involved a simple stripping procedure. First, a least-squares exponential was fitted to the slow component. The fit was then subtracted out and a least-squares exponential was fitted to the remaining current. For the amplitude of the fast component, we measured the amplitude of the current remaining after

TABLE I

Recording Solutions

External solutions*	Na	Ca	Ba	Mg	Mn	Tris	HEPES‡	Glucose
(A)	135	10	—	—	—	—	10	10
(B)	135	10	—	—	—	—	10	—
(C)	135	—	10	—	—	—	10	10
(D)	—	10	—	—	—	145	—	—
(E)	135	1	—	9	—	—	10	—
(F)	120	10	—	—	10	—	10	—

Internal solutions	Cs	NMG§	TEA‖	Na	Cl	F	Glu¶	EGTA**	HEPES**
(G)	135	—	—	—	30	25	80	10	10
(H)	105	—	—	30	30	25	80	10	10
(I)	85	30	20	—	20	20	95	—	10
(J)	135	—	—	—	30	—	105	10	10

*Concentrations are in millimolar.

‡External pH adjusted to pH 7.4 with NaOH.

§*N*-methyl-D-glucamine.

‖Tetraethylammonium.

¶Glutamate.

**EGTA and HEPES acid were neutralized (to pH 7.15) with CsOH.

subtraction of the slow exponential, rather than using the initial amplitude of the fitted fast exponential, because the possibility for extrapolation error was large. The amplitude of the slow component was taken as the initial amplitude of the fitted slow exponential.

RESULTS

RHPA Used to Characterize Secretion from Individual B Cells

Rat pancreatic B cells were identified and their secretion was characterized using the RHPA. This assay was developed by Neill and Frawley (1983) to study prolactin secretion from individual pituitary cells. In the assay, protein A–coupled SRBC are mixed with dispersed endocrine cells and the mixture is plated as a monolayer. The

cells are then incubated with antibody to the hormone of interest, which binds to protein A. Hormone secreted by an endocrine cell binds to antibody and activates complement-induced lysis of the SRBC. The lysed SRBC form a clearly visible "plaque" surrounding the endocrine cell. Fig. 1 shows several plaques formed by insulin-secreting B cells. The dark area surrounding individual B cells corresponds to the ghosts of SRBC that have undergone complement-induced lysis. Insulin-secreting B cells are clearly identified by this assay, so that cells used in patch-clamp experiments can be unambiguously identified. The cells illustrated in Fig. 1 are typical of those used in our experiments. The average diameter of the B cells was

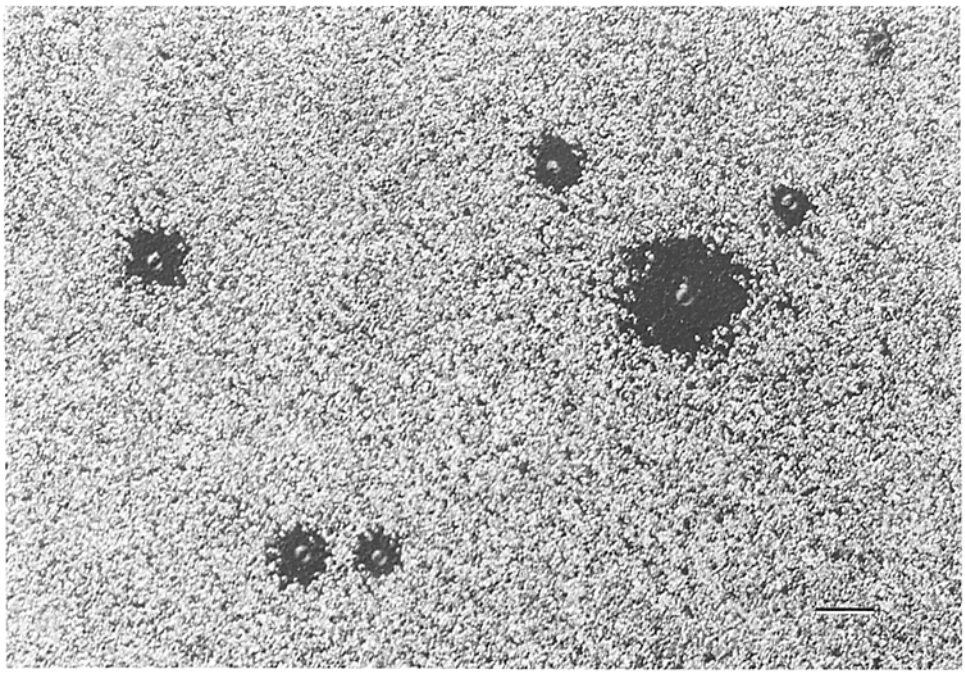

FIGURE 1. B cell plaques. The dark regions are hemolytic plaques, which were formed with 20 mM glucose used as insulin secretagogue in the presence of insulin antibody and complement. Near the center of each plaque is an insulin-secreting B cell, which can clearly be identified by this procedure. The photograph was taken through Nomarski differential interference contrast optics. The scale corresponds to 50 μm.

13.3 ± 2.4 μm. In control experiments, we found that if insulin antiserum or complement was omitted, plaques were not formed. In addition, if the SRBC were not coated with protein A, plaques were not formed.

We used the RHPA to characterize insulin secretion from single B cells by measuring two parameters. First, the percentage of cells that formed plaques was measured. This corresponds to the percentage of cells that secreted a detectable amount of insulin. Second, we measured the plaque area from secreting cells, which is proportional to the amount of insulin secreted (cf. Smith et al., 1986). Both the

percentage of plaque-forming cells and the plaque area increased as the glucose concentration was raised, as shown in Fig. 2. Fig. 2 *A* plots the percentage of plaque-forming cells as a function of the glucose concentration. In the absence of glucose, 13.2 ± 5.7% of the islet cells secreted insulin. As the glucose concentration was raised, the percentage of insulin-secreting cells increased and reached a maximum of 66.4 ± 12% at 20 mM glucose. In an attempt to estimate the percentage of insulin-secreting B cells in our cultures, we enhanced glucose-induced insulin release with the phosphodiesterase inhibitor IBMX, which is thought to increase secretion by raising intracellular cAMP (cf. Malaisse and Malaisse-Lagae, 1984). In

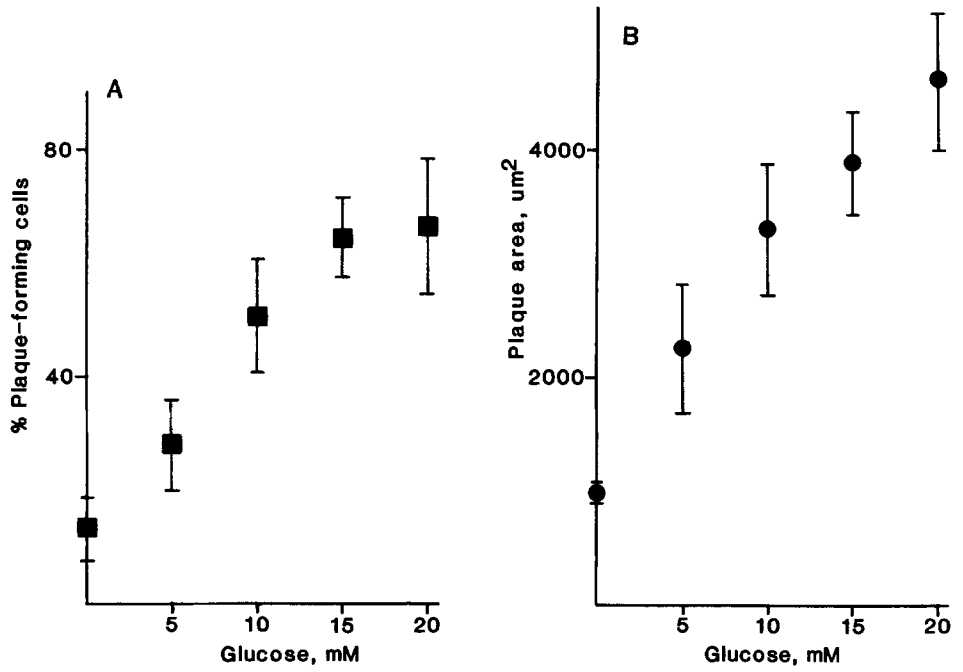

FIGURE 2. Insulin secretion measured with the RHPA. (*A*) Data points are means ± SD from four experiments. On the average, 230 cells were counted for each glucose concentration in each experiment. (*B*) Data points are means ± SEM from three experiments. On the average, 47 plaque areas were measured for each glucose concentration in each experiment.

two experiments in which 1 mM IBMX was included with 20 mM glucose, the percentage of insulin-secreting cells was 83 and 95%. This was the maximum stimulation we achieved, and it would place an upper limit on the percentage of secreting B cells in our cultures. It can be seen clearly in Fig. 1 that plaque area, and thus insulin secretion, is variable from cell to cell. This appears to be a common feature of secretion in endocrine cells (Smith et al., 1986). Plaque area as a function of glucose concentration is plotted in Fig. 2 *B*. In our experiments, plaque area ranged from 963 ± 123 μm^2 (mean ± SEM) in the absence of glucose to 4,605 ± 612 μm^2 in 20 mM glucose.

Na Channels in B Cells

Previous reports have indicated that only a small fraction of mouse and neonatal rat B cells contain Na channels (Satin and Cook, 1985; Rorsman and Trube, 1986). However, we have found that nearly all of the identified adult rat B cells we studied had a transient inward current component that was identified as Na current. Fig. 3 *A* illustrates a family of whole-cell currents exhibiting the transient component. The

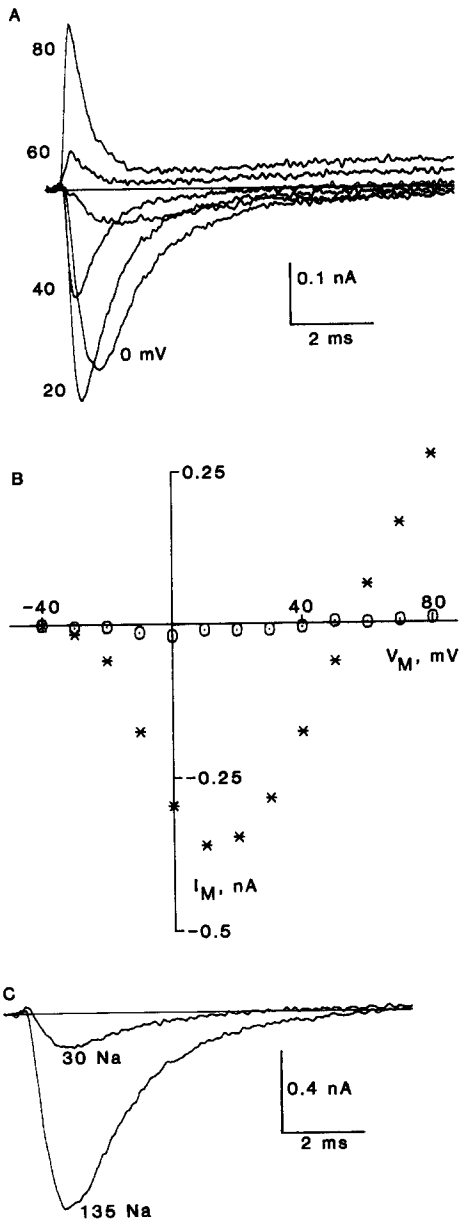

FIGURE 3. Na currents and the Na current-voltage relationship. (*A*) The illustrated currents were recorded during 10-ms steps to the indicated voltages, from a holding potential of −80 mV. (*B*) The peak Na current is plotted as a function of voltage under control conditions (asterisks) and after adding 200 nM TTX (circles). *A* and *B* are from the same cell in experiment OC086A using external solution A and internal solution H. (*C*) Currents recorded during 10-ms steps to 0 mV. The control trace was obtained in external solution B, and then the smaller current was recorded from the same cell after reducing the external Na concentration to 30 mM (by isotonic substitution of Tris for Na). Experiment DE037A using internal solution G.

currents rapidly activate to a peak and then inactivate during maintained depolarization. The transient current reverses direction from inward to outward between +40 and +60 mV. The peak current-voltage relationship for this current (Fig. 3 *B*) illustrates that the current first becomes activated at about −30 mV and reaches a maximum near +10 mV. This early transient current is blocked by 200 nM tetrodotoxin (TTX) (Fig. 3 *B*) and its magnitude is decreased when the external Na concentration is reduced (Fig. 3 *C*), which indicates that it is carried by voltage-dependent Na channels. In 11 cells, the maximum magnitude of the Na current was 0.21 ± 0.10 nA.

Steady State Inactivation of Na Channels

Rat B cell Na channels inactivate over a relatively negative voltage range. Steady state inactivation of Na channels was determined with the following pulse protocol: a

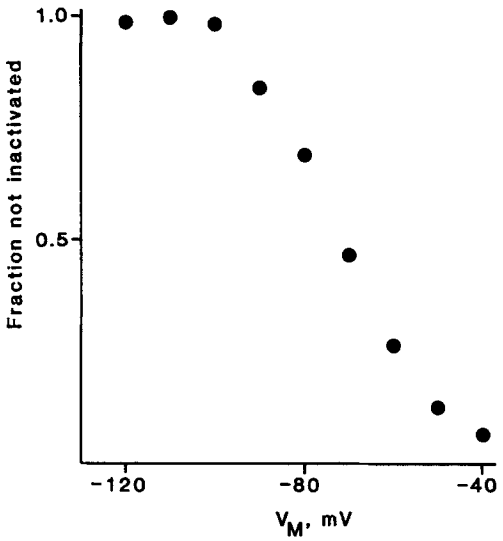

FIGURE 4. Voltage dependence of Na current inactivation. A 50-ms prepulse was used to inactivate Na channels to a steady state level. The Na current recorded during a subsequent test pulse to +10 mV was used to determine the fraction of noninactivated channels. The magnitude of the current during the test pulse was normalized and plotted as a function of prepulse voltage in this figure. Experiment NO136A. External solution B and internal solution H.

50-ms prepulse to various voltages was used to inactivate Na channels to a steady state level, and a subsequent test pulse to +10 mV was used to assess the number of noninactivated channels. The steady state inactivation curve obtained in this way is shown in Fig. 4. Inactivation becomes apparent at −90 mV and is nearly complete at −40 mV.

Some previous studies, utilizing microelectrode recording techniques, have concluded that Na channels are not involved in B cell electrical activity (Meissner and Schmelz, 1974; Ribalet and Beigelman, 1982). This conclusion was based in part on the fact that TTX did not affect the pattern of electrical activity. The present demonstration that Na channels are present in B cells is not inconsistent with these previous reports, when the steady state inactivation curve shown in Fig. 4 is considered. Microelectrode recordings have shown that the plateau potential, from which B cell spikes originate, is near −40 mV (Meissner, 1976). At this voltage, most

Na channels in rat B cells would be inactivated, and blocking the channels with TTX could not be expected to have an effect on electrical activity.

TTX Inhibits Secretion from B Cells

Because of the presence of Na channels in B cells, we decided to investigate the effect of TTX on insulin secretion using the RHPA. In each of three experiments, we found an effect of TTX on both the percentage of plaque-forming cells and on the plaque area. Therefore, to get an overall measure of the insulin secretion from a population of cells, we multiplied the average plaque area by the percentage of plaque-forming cells. The results of the three experiments on the effect of TTX are presented in Table II. To test for significant effects, we performed a two-factor analysis of variance with interaction in the model (Kempthorne and Folks, 1971). This analysis showed that insulin secretion is significantly affected by both the glucose concentration ($P < 0.001$) and the presence of TTX ($P < 0.001$). Furthermore, there are significant interactions between glucose and TTX ($P < 0.001$); i.e., the effect of TTX depends

TABLE II

Effect of TTX on Insulin Secretion at Different Glucose Concentrations

Glucose concentration	0 mM	5 mM	10 mM	15 mM	20 mM
No TTX	102.2*	634.8	1,611.9	2,422.1	3,093.6
	101.4	570	1,193.6	2,543.2	2,567.9
	94.43	616.8	2,055.45	2,682.7	3,322.7
200 nM TTX	94.99	693.45	1,064.5	1,352.7	1,051.3
	71.32	259.7	474.08	1,289.9	1,386.1
	108.04	740.2	942.9	1,872.9	1,412.7

*The three numbers for each experimental condition are measurements from three separate experiments. The measure of insulin secretion is the percentage of plaque-forming cells times the average plaque area from secreting cells.

on the glucose concentration. These results are clearly illustrated by the plots of these data shown in Fig. 5. Increasing the glucose concentration increases insulin secretion, as measured by the RHPA; TTX has little or no effect on secretion at 0 or 5 mM glucose, but inhibits insulin secretion at glucose concentrations of 10–20 mM.

Ca Currents Are Carried by Two Types of Ca Channels in B Cells

In whole-cell patch-clamp experiments, many cells exhibited a maintained inward current that was TTX insensitive. This current is illustrated in Fig. 6, which shows currents during steps to +20 mV in the absence or presence of 200 nM TTX. A steady inward current remains after the Na current has inactivated (Fig. 6 *A*). The maintained inward current is TTX insensitive (Fig. 6 *B*) and, as demonstrated below, is carried by voltage-dependent Ca channels. After repolarization, the Ca current "tail" decays in two phases. At 20–22°C and −80 mV, the time constant of the fast component of the tail current averaged 129 ± 42 μs and that of the slow component was 2.8 ± 0.44 ms in 16 cells.

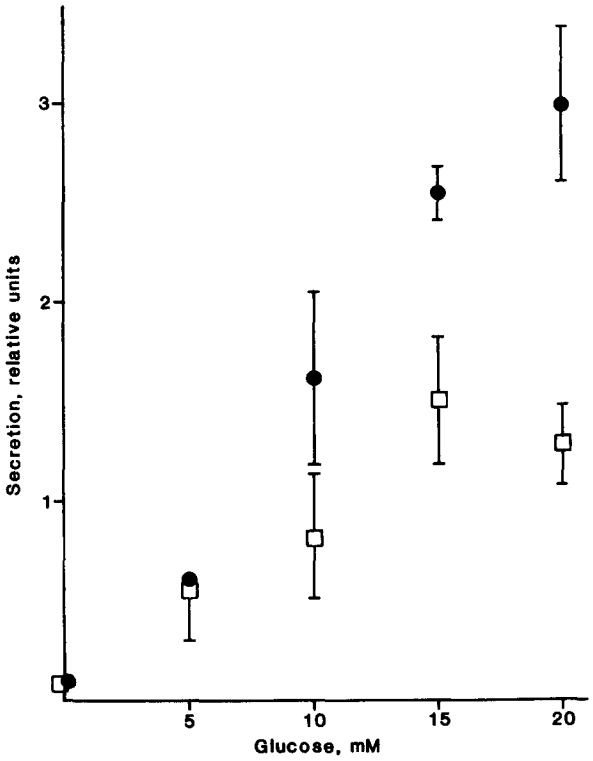

FIGURE 5. TTX partially inhibits glucose-induced insulin secretion. The overall secretory activity of a population of B cells was estimated by multiplying the average plaque area formed by secreting cells by the percentage of plaque-forming cells. This measure of secretion is plotted vs. glucose concentration in the figure. Data points are means ± SD from three experiments. Circles: control, in the absence of TTX; squares: secretion in the presence of 200 nM TTX.

We have identified the macroscopic currents illustrated in Fig. 6 *B* as Ca currents in a number of ways. First, to test for the possibility that any of the TTX-insensitive inward current is carried by external Na, we replaced Na with Tris. Tris substitution for Na did not change the inward current pattern (Fig. 7 *A*), and both fast and slow

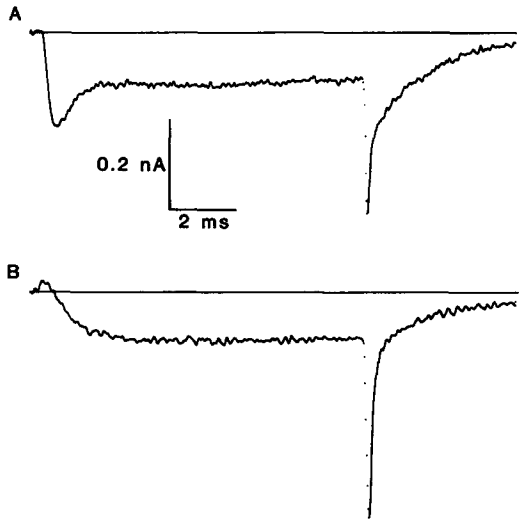

FIGURE 6. TTX-insensitive inward currents have both a fast and a slow phase of deactivation. In both *A* and *B*, a 10-ms step to +20 mV was applied from a holding potential of −80 mV. (*A*) In the absence of TTX, Na current is apparent at the beginning of the depolarization. After repolarization, the tail current decays in two exponential phases with time constants of 93.3 μs and 1.98 ms. Experiment OC086A. External solution A and internal solution G. (*B*) In the presence of TTX, the tail current still decays in two phases, in this case with time constants of 116 μs and 2.40 ms. Experiment OC296A. External solution A plus 200 mM TTX and internal solution I.

components of the tail current were present. Second, both tail currents were reduced in magnitude when the external Ca concentration was decreased (by substituting Mg for Ca), as shown in Fig. 7 *B*. Finally, inorganic Ca channel blockers decreased both tail current components (Fig. 7 *C*). Thus, there is no doubt that both the fast and slow phases of tail current reflect the activity of Ca channels.

In Fig. 7, *B* and *C*, some tail current remains after interventions that appear to abolish the inward current during the depolarization. Two factors support the idea that the remaining tail currents are carried by Ca channels. First, we believe that the inward current during the pulse is partially obscured by a nonlinear leak current. In Fig. 7 *B*, for example, the initial outward current hump is probably an artifact of our linear leak subtraction procedure. Thus, the small inward Ca current is superimposed on a steady outward leakage current. Second, high concentrations of inorganic Ca

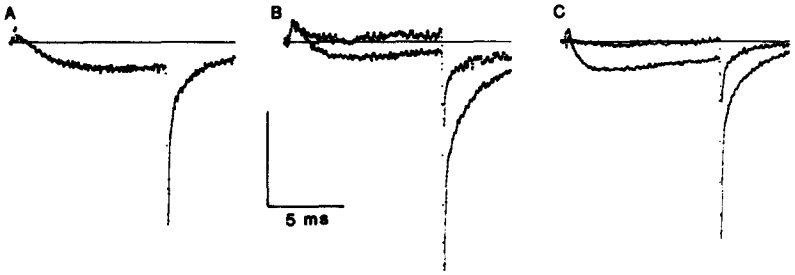

FIGURE 7. Identification of TTX-insensitive currents as Ca currents. All currents in this figure were generated by 10-ms steps to +40 mV from a holding potential of −80 mV, using internal solution G. 200 nM TTX was present externally. The vertical scale corresponds to 0.25 nA in *A* and *B*, and 0.5 nA in *C*. (*A*) Current recorded in external solution D, containing only 145 mM Tris, 10 mM Ca, and 200 nM TTX. Both fast and slow tail current components are present, indicating that neither is the result of Na permeation through K or other channel types. Experiment MR277A. (*B*) A decrease in external Ca reduces both the fast and the slow tail components. The larger (control) trace is the average of records taken in external solution B (containing 10 mM Ca) before and after recording the smaller experimental trace in solution E containing 1 mM Ca. Experiment AP087A. (*C*) Mn ions inhibit both the fast and the slow tail currents. The larger trace is the average of records taken in external solution B before and after recording the smaller current in solution F. Experiment MR137A.

channel blockers completely blocked the tail currents, lending further support to the idea that all of the tail current flows through Ca channels.

The pattern of inward macroscopic currents that we have just described in pancreatic B cells is very similar to that previously found in GH3 anterior pituitary cells (Armstrong and Matteson, 1985; Cohen and McCarthy, 1985). In GH3 cells, the two components of tail current reflect the activity of two distinct populations of Ca channels, which were called SD (for slowly deactivating) and FD (for fast deactivating) Ca channels. In light of the apparent similarity between B cell and GH3 cell Ca currents, we have examined the properties of tail currents in B cells in some detail in an attempt to determine whether two Ca channel types are present. The following sections illustrate that, in addition to their different rates of deactivation, the two components differ in activation range, inactivation, Ca/Ba selectivity, and sensitivity

to washout. As a result, we conclude that B cells have both SD and FD Ca channels with properties very similar to the two populations of Ca channels in GH3 cells.

Voltage Dependence of Ca Currents

One of the ways in which separate populations of Ca channels differ is in their activation voltage ranges. The presence of a shoulder in the Ca current-voltage relationship has been used to demonstrate this voltage separation (e.g., Nowycky et al., 1985; Cota, 1986). However, the current-voltage relationship in B cells does not have a prominent shoulder (Fig. 8). The position of the current-voltage curve shown in Fig. 8 is representative of several we have constructed from identified B cells. Ca current first becomes detectable at about −40 mV and reaches a maximum at 0 to +10 mV. The maximum magnitude of the Ca current is variable from cell to cell, ranging from as little as 10–20 pA to as much as 350 pA.

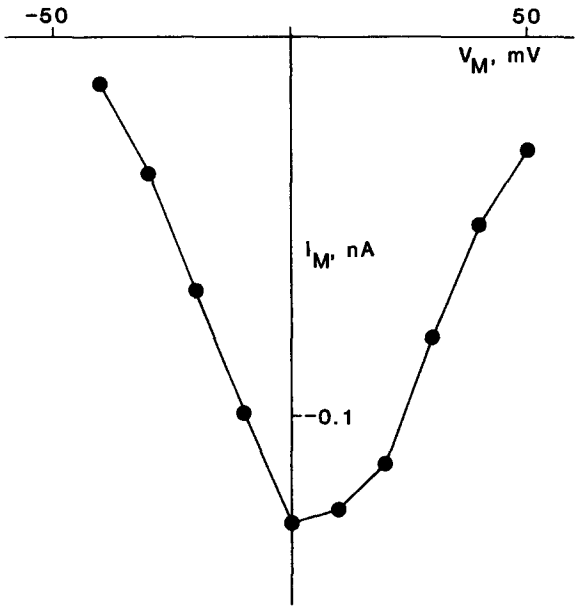

FIGURE 8. Ca current-voltage relationship. The maximum magnitude of inward current during 10-ms steps is plotted as a function of step voltage. Experiment OC296A. External solution A plus 200 nM TTX and internal solution I.

In order to determine the voltage range over which the two Ca channel types activate, one can take advantage of the order-of-magnitude difference in channel deactivation kinetics to separate fast and slow tail current components as described in the Methods. The data for Fig. 9 were obtained by recording tail currents following 10-ms steps to various voltages. Fig. 9 plots the normalized fast and slow tail current amplitudes as a function of the voltage during the preceding step. The resulting plots demonstrate that the slow tail current component (labeled "SD channels" in Fig. 9) activates over a more negative voltage range than the fast component ("FD channels"). SD channels begin to activate near −40 mV, whereas the FD channel current first turns on near −20 mV. Half-maximum activation is near −5 mV for SD channels and near +15 mV for FD channels.

Inactivation

The two Ca current components differ in their inactivation properties. The slow component inactivates rapidly and the fast one inactivates little during a 100-ms depolarization. This was demonstrated by measuring Ca tail currents after depolarizing pulses of varying durations. Fig. 10 *A* shows two superimposed tail currents that followed either 10- or 100-ms steps to +20 mV. After the 10-ms step, the tail current obviously decays in two phases: there is a prominent slow component as well as a fast phase of decay. However, after the 100-ms step, the slow component is nearly abolished and the tail current has mainly a fast decay phase. The slow component

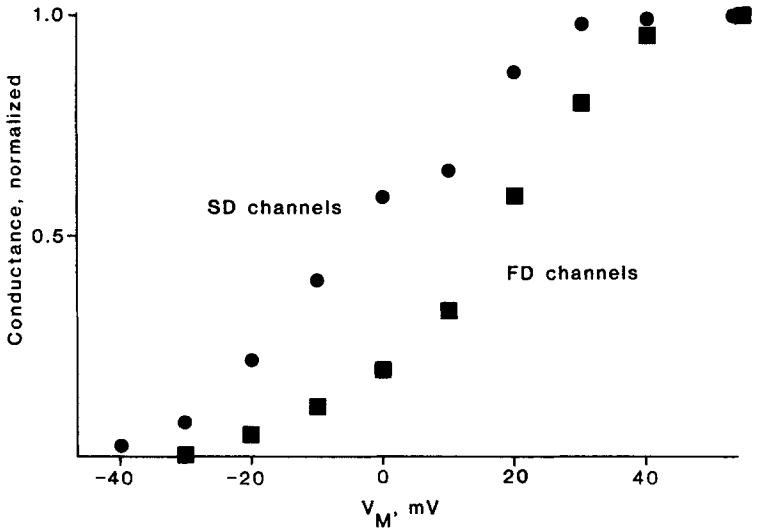

FIGURE 9. Fast and slow tail current components activate over different voltage ranges. Ca tail currents were measured following 10-ms voltages-clamp steps to various potentials. The fast and slow components of the tail were separated as described in the Methods. The normalized amplitudes of the fast tail current (labeled FD channels) and slow tail current (SD channels) were averaged from six cells and the averages are plotted in the figure. Experiments OC296A, OC306A, OC306B, and OC316A. External solution A plus 200 nM TTX and internal solution I.

disappears as the SD channels become inactivated during the depolarization. The time course of inactivation can be illustrated by plotting the amplitudes of the two tail current components as a function of pulse duration, as shown in Fig. 10 *B*. These plots illustrate that although the slow component of tail current is nearly abolished after a 75–100-ms depolarization, the fast component remains virtually unchanged. This is consistent with the notion that the slow component of the tail reflects the activity of a population of channels (SD channels) that inactivate during maintained depolarization. FD channels, on the other hand, do not inactivate during a 100-ms pulse.

Selectivity

The relative ability of each population of Ca channels to conduct Ca^{2+} or Ba^{2+} was used as a measure of channel selectivity. We tested the ability of FD and SD channels to conduct divalent cations by measuring the amplitude of the fast and slow Ca tail currents, as shown in Fig. 11. Because Ca or Ba ions might differ in their ability to

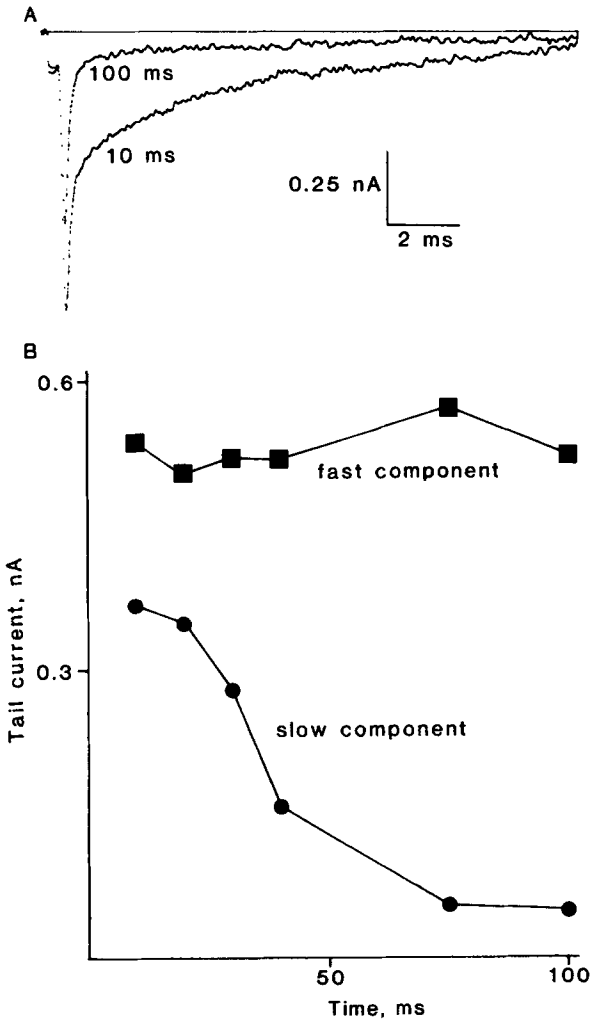

FIGURE 10. Inactivation of Ca tail currents. (*A*) Two Ca tail currents are superimposed. The currents were recorded following a 10-ms or a 100-ms step to +20 mV. (*B*) The fast and slow tail current components were separated as described in the Methods and are plotted as a function of prepulse duration. Experiment OC306B. External solution A plus 200 nM TTX and internal solution I.

cause voltage shifts in channel gating (cf. Kass and Krafte, 1987), we examined tail currents over a range of activating voltages. Fig. 11, *A* and *B*, shows tail currents that followed 10-ms steps to +60 mV, with either 10 mM Ca or 10 mM Ba present as the current carrier. At this positive activating voltage, the conductance-voltage relationship of both SD and FD channels has saturated (cf. Fig. 9), so the effect of different gating shifts would be minimized. It is clear that the amplitude of the slow component

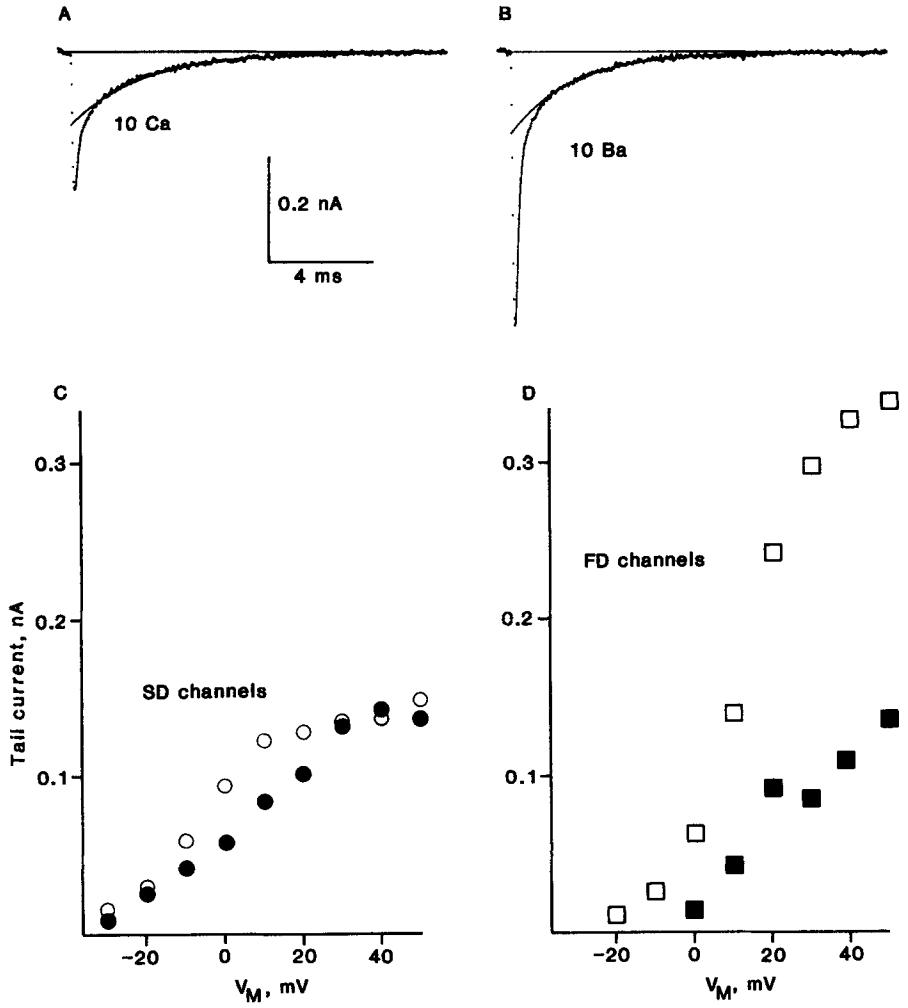

FIGURE 11. Ca/Ba selectivity of SD and FD channels. (*A* and *B*) Current tails recorded at −80 mV following 10-ms steps to +60 mV in external solution A (*A*) or external solution C (*B*), both containing 200 nM TTX. Exponential fits to the slow components of the tails are shown superimposed over the tail currents. For the plots shown in *C* and *D*, tail currents were recorded following 10-ms steps to various voltages, and the fast and slow tail current components were separated as described in the Methods. The conductance at the end of the 10-ms step is proportional to the tail current amplitude (assuming a linear current-voltage relationship), so the plots in *C* and *D* are scaled versions of the conductance-voltage relationship. (*C*) Slow tail current in 10 mM Ca (filled circles) or 10 mM Ba (open circles). (*D*) Fast tail current in 10 mM Ca (filled squares) or 10 mM Ba (open squares). All data are from a single cell in experiment JL147A. Internal solution J.

of the tail is about the same in 10 mM Ca as in 10 mM Ba. On the other hand, the fast component is over two times larger in 10 mM Ba as in 10 mM Ca. Examination of the conductance-voltage relationships shown in Fig. 11, *C* and *D*, clearly indicates that the maximum conductance of SD channels is the same with Ca^{2+} or Ba^{2+} as the current carrier, whereas the maximum conductance of FD channels is much larger in Ba^{2+} than in Ca^{2+}. In five cells, the ratio of the tail current amplitude in 10 mM Ba to that in 10 mM Ca averaged 1.00 ± 0.13 for SD channels and 2.25 ± 0.47 for FD channels.

Washout

It is well known that the Ca current amplitude declines relatively rapidly during intracellular perfusion (cf. Kostyuk, 1984). In some cells with more than one type of Ca channel, one form of the channel is resistant to channel "washout" (Nilius et al., 1985; Matteson and Armstrong, 1986; Cota, 1986). For example, in anterior

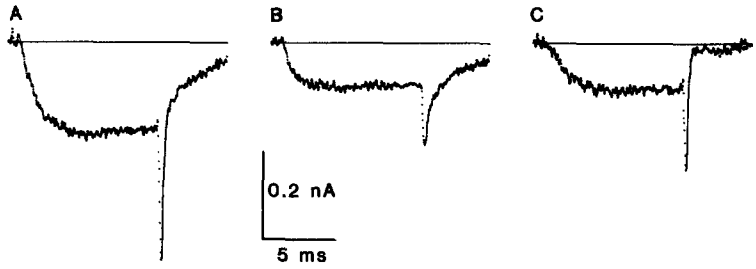

FIGURE 12. Washout of FD channels during intracellular dialysis. The currents shown in *A* and *B* were generated by 10-ms steps to +20 mV. (*A*) Current recorded shortly after rupturing the patch of membrane under the electrode tip, thereby breaking into the cell. (*B*) Current recorded 7 min after breaking into the cell. (*C*) Difference between the currents shown in *A* and *B*. Experiment DE047A. External solution B plus 200 nM TTX and internal solution G.

pituitary cells, it has been reported that in the absence of intracellular ATP, FD channels washout rapidly and SD channels are resistant to washout (Cota, 1986). This is also true in B cells, as shown in Fig. 12. The current generated by a 10-ms step to +20 mV shortly after breaking into the cell (Fig. 12 *A*) displays a steady state Ca component and both a fast and a slow Ca tail current. After 7 min of dialysis with an ATP-free pipette solution, the fast tail current and the steady state current during the pulse are greatly reduced (Fig. 12 *B*). The current that has washed out can be obtained by subtracting the late current from the earlier one. The resulting difference current (Fig. 12 *C*) is a slowly activating inward current during the depolarization, followed by a fast tail current during repolarization, which reflects the activity of FD channels. SD Ca channels are not significantly affected by the dialysis.

DISCUSSION

The major results presented in this article are the following. (*a*) We have demonstrated that the RHPA can be used to study insulin secretion from single B cells and

also to identify secreting B cells for electrophysiological experiments. (*b*) All rat B cells contain Na channels. Our results indicate that the Na channels are functionally important because the channel blocker TTX partially inhibits glucose-induced insulin secretion. (*c*) B cells contain two types of Ca channels with properties similar to the FD and SD Ca channels found in anterior pituitary cells.

Plaque Assay

We have shown that the RHPA is a useful technique for identifying and studying secretion from individual pancreatic B cells. In other laboratories studying electrophysiological properties of isolated B cells, identification of the cell type often involves testing for glucose-induced electrical activity. However, since electrical activity in other pancreatic islet cell types has not been fully described, it is possible that this identification could result in false positives. An advantage of the RHPA is that B cells can be unambiguously identified. Another immunological approach to identifying B cells involved the use of immunocytochemistry after patch-clamp recording (Cook et al., 1984). A second advantage of the RHPA is that one has an indication of the secretory activity of the B cell that is being studied electrophysiologically. This could be important when attempting to correlate the effect of a chemical agent (i.e., a primary secretagogue, neurotransmitter, or hormone) on insulin secretion with its effect on channel activity. A final advantage of the RHPA is that it can also be used to identify glucagon-secreting A cells and somatostatin-secreting D cells for electrophysiological studies.

Salomon and Meda (1986) have also used the RHPA to study insulin secretion from B cells. They reported that single B cells exhibited a 1.7-fold increase in plaque area when the glucose concentration was raised from 2.8 to 16.7 mM. That increase was less than the fourfold increase in plaque area that we find when glucose was raised from 0 to 15 mM. This discrepancy may have resulted from the somewhat different conditions used in the RHPA. We have also measured a more complete dose-response curve for glucose-stimulated insulin secretion from single B cells (Figs. 1 and 5). The dose-response curves shown in Fig. 5 are sigmoid in shape and resemble those measured from intact islets (e.g., Ashcroft et al., 1972). This demonstrates that the RHPA provides an accurate measure of insulin secretion from isolated, single B cells.

Several laboratories have recently demonstrated that the RHPA is a simple, useful technique for identifying specific cell types for patch-clamp experiments (Lingle et al., 1986; DeRiemer and Sakmann, 1986; Gregerson and Oxford, 1987). These other studies have involved the identification of specific subpopulations of anterior pituitary cells. Gregerson and Oxford (1987) have specifically tested for effects of the assay procedure itself on the ionic channels under study. They compared the properties of channels in GH3 cells that had undergone the RHPA with channels in control cells and concluded that the assay has little or no effect. We also recorded from islet cells that were not subjected to the RHPA and these cells exhibited the same current components found in RHPA-identified B cells.

Na Channels in B Cells

The presence of voltage-dependent Na channels in B cells has been a controversial question in recent years. Several reports have indicated that glucose-induced

electrical activity is not affected by TTX (Dean and Matthews, 1970; Meissner and Schmelz, 1974), and it was therefore concluded that Na channels were not involved in either plateau or spike generation. In agreement, some recent patch-clamp studies of mouse (Rorsman and Trube, 1986) and neonatal rat (Satin and Cook, 1985) B cells have indicated that few B cells generate Na currents. On the other hand, it has been reported that veratridine, which opens Na channels in nerve, depolarizes rat B cells, and the depolarization is blocked by TTX (Pace, 1979). We believe that a likely explanation for the lack of demonstrable Na channels in earlier microelectrode studies is due to the fact that the channels are mostly inactivated at the voltages where spiking is recorded. It seems possible that the recorded values of membrane potential are less negative than the true values occurring in normal, intact B cells, because of damage caused by microelectrode impalement. Thus, functional Na channels may in fact be present in all B cells. Another possibility, which would explain the differences between our results and those of Rorsman and Trube (1986), is that rat B cells have Na channels and mouse B cells do not.

We have also shown that the Na channels in rat B cells are functionally important for stimulus-secretion coupling. This was demonstrated by using the RHPA to show that TTX partially inhibits glucose-induced insulin secretion. TTX had no significant effect at, or below, 5 mM glucose, which is near the threshold for activating electrical activity (Meissner and Schmelz, 1974). At higher glucose concentrations, TTX clearly inhibited secretion (Fig. 5). Others have also shown that TTX had a small but significant inhibitory effect on glucose-induced insulin secretion from perfused rat islets (Donatsch et al., 1977). The effect of TTX on secretion suggests that Na channels are partly responsible for depolarizing the B cell and thereby activating voltage-dependent Ca channels.

Comparison of Rat B Cell Ca Channel Properties with the Literature

At least two discrete populations of Ca channels have now been found in a variety of cell types, including clonal anterior pituitary cells (Armstrong and Matteson, 1985; Cohen and McCarthy, 1985; Matteson and Armstrong, 1986), cells of the pars intermedia of the rat pituitary (Cota, 1986), vertebrate neurons (Carbone and Lux, 1984; Nowycky et al., 1985), neuroblastoma cells (Narahashi et al., 1987), vertebrate heart (Bean, 1985; Nilius et al., 1985), skeletal muscle (Cota and Stefani, 1985), and vascular smooth muscle (Sturek and Hermsmeyer, 1985). The two forms of the Ca channel reported here in rat pancreatic B cells are very similar to the two types described in anterior pituitary cells. The properties of SD and FD Ca channels in B cells are qualitatively the same as in GH3 cells. In both cell types, SD channels deactivate more slowly, they activate over a more negative voltage range, they inactivate faster, and they are more resistant to washout than FD channels (cf. Matteson and Armstrong, 1986). The same two Ca channel types, with nearly identical properties, also appear in normal, adult pituitary cells (Cota, 1986). These two populations of Ca channels found in endocrine cells are similar in many respects to, and may in fact be the same as, T- and L-type Ca channels found in other cells. For example, in vertebrate heart, the T channel activates at more negative voltages and inactivates faster than the L channel (Nilius et al., 1985). In addition, the T channel remains functional after patch excision, whereas the L channel irreversibly disap-

pears. Thus, the T channel is similar to our SD channels and the L channel is similar to FD channels.

Ca currents have been described in several B cell preparations, including neonatal rats (Satin and Cook, 1985), NMRI mice (Rorsman and Trube, 1986), HIT cells (Matteson and Matschinsky, 1986), and RINm5F cells (Findlay and Dunne, 1985). In addition to our data, the most detailed study of Ca channels in B cells was by Rorsman and Trube, whose data suggest a single population of Ca channels that are most like our FD channels. Rorsman and Trube (1986) reported that Ca tail currents could be fitted by a single exponential with a time constant of 180 μs at -70 mV, which is similar to our FD tail current component. In addition, their Ca currents inactivate little during 200-ms depolarizations, which is also FD-like. Their Ca channels were half-maximally activated at $+4$ mV in 10 mM Ca, which is halfway between half-maximal activation of SD and FD channels in rat B cells (cf. Fig 9).

Possible Functions of SD and FD Ca Channels

The two populations of Ca channels in B cells might provide an explanation for much of the complex pattern of electrical activity in these cells. There is evidence that the prolonged plateau depolarization in B cells is a voltage-dependent action potential (Cook et al., 1980). Microelectrode studies have shown that Ca channel blockers inhibit the plateau depolarization, but TTX has no effect, which suggests that Ca channels are involved (Ozawa and Sand, 1986). SD Ca channels are most likely to be involved in generating the plateau depolarization because of their more negative activating voltage. SD channels might initiate the plateau depolarization, but they would inactivate relatively quickly and thus not carry inward current throughout the entire duration of the plateau. Termination of the plateau is probably determined by a number of factors, including activation of Ca-activated K channels. FD channels, with their more positive activation range, would probably be responsible for generating the spikes that are superimposed on the plateau depolarization. It should be pointed out that the voltage range over which the Ca channels activate under physiological conditions is probably somewhat more negative than that shown in Fig. 9. Our conductance-voltage curves were measured in the presence of 10 mM Ca, which is substantially higher than physiological Ca levels. The higher extracellular Ca would be expected to shift the activation curve in the depolarizing direction (e.g., Kass and Krafte, 1987).

We would like to thank Stephen Frawley for invaluable assistance in setting up the B cell plaque assay. We would also like to thank Carol Deutsch for providing some support and laboratory space for performing some of the secretion studies.

This work was supported by National Institutes of Health grant DK-33212 to D.R. Matteson from the National Institute of Diabetes and Digestive and Kidney Diseases.

Original version received 25 August 1987 and accepted version received 4 January 1988.

REFERENCES

Armstrong, C. M., and F. Bezanilla. 1974. Charge movement associated with the opening and closing of the activation gates of the Na channel. *Journal of General Physiology.* 63:533–552.

Armstrong, C. M., and D. R. Matteson. 1985. Two distinct populations of calcium channels in a clonal line of pituitary cells. *Science.* 227:65–67.

Ashcroft, S. J. H., J. M. Bassett, and P. J. Randle. 1972. Insulin secretion mechanisms and glucose metabolism in isolated islets. *Diabetes.* 21:538–545.

Ashcroft, F. M., D. E. Harrison, and S. J. H. Ashcroft. 1984. Glucose induces closure of single potassium channels in isolated rat pancreatic B-cells. *Nature.* 312:446–448.

Bean, B. P. 1985. Two kinds of calcium channels in canine atrial cells. Differences in kinetics, selectivity, and pharmacology. *Journal of General Physiology.* 86:1–30.

Carbone, E., and H. D. Lux. 1984. A low voltage-activated, fully inactivating Ca channel in vertebrate sensory neurons. *Nature.* 310:501–502.

Cohen, C. J., and R. T. McCarthy. 1985. Differential effect of dihydropyridines on two populations of Ca channels in anterior pituitary cells. *Biophysical Journal.* 47:513*a*. (Abstr.)

Cook, D. L., W. E. Crill, and D. Porte, Jr. 1980. Plateau potentials in pancreatic islet cells are voltage-dependent action potentials. *Nature.* 286:404–406.

Cook, D. L., M. Ikeuchi, and W. Y. Fujimoto. 1984. Lowering of pHi inhibits Ca^{2+}-activated K channels in pancreatic B-cells. *Nature.* 311:269–271.

Cota, G. 1986. Calcium channel currents in pars intermedia cells of the rat pituitary gland. Kinetic properties and washout during intracellular dialysis. *Journal of General Physiology.* 88:83–105.

Cota, G., and E. Stefani. 1985. Fast and slow calcium channels in twitch muscle fibers of the frog. *Biophysical Journal.* 47:65*a*. (Abstr.)

Dean, P. M., and E. K. Matthews. 1968. Electrical activity in pancreatic islet cells. *Nature.* 219:389–390.

Dean, P. M., and E. K. Matthews. 1970. Glucose-induced electrical activity in pancreatic islet cells. *Journal of Physiology.* 210:255–264.

Dean, P. M., E. K. Matthews, and Y. Sakamoto. 1975. Pancreatic islet cells: effects of monosaccharides, glycolytic intermediates and metabolic inhibitors on membrane potential and electrical activity. *Journal of Physiology.* 246:459–478.

DeRiemer, S. A., and B. Sakmann. 1986. Two calcium currents in normal rat anterior pituitary cells identified by a plaque assay. *In* Calcium Electrogenesis and Neuronal Functioning. U. Heinemann, M. Klee, E. Neher, and W. Singer, editors. Springer-Verlag, Heidelberg. 139–154.

Donatsch, P., D. A. Lowe, B. P. Richardson, and P. Taylor. 1977. The functional significance of sodium channels in pancreatic beta-cell membranes. *Journal of Physiology.* 267:357–376.

Findlay, I., and M. J. Dunne. 1985. Voltage-activated Ca^{2+} currents in insulin-secreting cells. *FEBS Letters.* 189:281–285.

Gregerson, K. A., and G. S. Oxford. 1987. Comparison of ionic currents in normal and reverse hemolytic plaque-identified rat pituitary cells under voltage clamp. *Biophysical Journal.* 51:431*a*. (Abstr.)

Hamill, O. P., A. Marty, E. Neher, B. Sakmann, and F. J. Sigworth. 1981. Improved patch-clamp techniques for high-resolution current recording from cells and cell-free membrane patches. *Pflügers Archiv.* 391:85–100.

Hiriart, M., and D. R. Matteson. 1987. Patch clamp study of ionic channels in rat pancreatic B-cells identified with the reverse hemolytic plaque assay. *Biophysical Journal.* 51:250*a*. (Abstr.)

Kass, R. S., and D. S. Krafte. 1987. Negative surface charge density near heart calcium channels. Relevance to block by dihydropyridines. *Journal of General Physiology.* 89:629–644.

Kempthorne, O., and L. Folks. 1971. Probability, Statistics, and Data Analysis. Iowa State University Press, Ames, IA. 470–481.

Kostyuk, P. G. 1984. Metabolic control of ionic channels in the neuronal membrane. *Neuroscience.* 13:983–989.

Lacy, P. E., and M. D. Kostianovsky. 1967. Method for the isolation of intact islets of Langerhans from the rat pancreas. *Diabetes.* 16:35-39.

Lingle, C. J., S. Sombati, and M. E. Freeman. 1986. Membrane currents in identified lactotrophs of rat anterior pituitary. *Journal of Neuroscience.* 6:2995–3005.

Malaisse, W. J., and F. Malaisse-Lagae. 1984. The role of cyclic AMP in insulin release. *Experientia.* 40:1068–1084.

Matteson, D. R., and C. M. Armstrong. 1984. Na and Ca channels in a transformed line of anterior pituitary cells. *Journal of General Physiology.* 83:371–394.

Matteson, D. R., and C. M. Armstrong. 1986. Properties of two types of calcium channels in clonal pituitary cells. *Journal of General Physiology.* 87:161–182.

Matteson, D. R., and F. M. Matschinsky. 1986. Identification of several types of voltage and/or Ca activated channels in a pancreatic beta cell line. *Biophysical Journal.* 49:432*a*. (Abstr.)

Meda, P., E. L. Hooghe-Peters, and R. Orci. 1980. Monolayer cultures of adult pancreatic islet cells on osmotically disrupted fibroblasts. *Diabetes.* 29:497–500.

Meissner, H. P. 1976. Electrical characteristics of the beta-cells in pancreatic islets. *Journal de Physiologie.* 72:757–767.

Meissner, H. P., and I. J. Atwater. 1976. The kinetics of electrical activity of beta cells in response to a "square wave" stimulation with glucose or glibenclamide. *Hormone and Metabolism Research.* 8:11–16.

Meissner, H. P., and H. Schmelz. 1974. Membrane potential of beta cells in pancreatic islets. *Pflugers Archiv.* 351:195–206.

Misler, S., L. C. Falke, K. Gillis, and L. McDaniel. 1986. A metabolite-regulated potassium channel in rat pancreatic B cells. *Proceedings of the National Academy of Sciences.* 83:7119–7123.

Narahashi, T., A. Tsunoo, and M. Yoshii. 1987. Characterization of two types of calcium channels in mouse neuroblastoma cells. *Journal of Physiology.* 383:231–249.

Neill, J. D., and L. S. Frawley. 1983. Detection of hormone release from individual cells in mixed populations using a reverse hemolytic plaque assay. *Endocrinology.* 112:1135–1137.

Nilius, B., P. Hess, J. B. Lansman, and R. W. Tsien. 1985. A novel type of cardiac calcium channel in ventricular cells. *Nature.* 316:443–446.

Nowycky, M. C., A. P. Fox, and R. W. Tsien. 1985. Three types of neuronal calcium channel with different calcium agonist sensitivity. *Nature.* 316:440–443.

Ozawa, S., and O. Sand. 1986. Electrophysiology of excitable endocrine cells. *Physiological Reviews.* 66:887–952.

Pace, C. S. 1979. Activation of Na channels in islet cells: metabolic and secretory effects. *American Journal of Physiology.* 237:E130–E135.

Ribalet, B., and P. M. Beigelman. 1980. Calcium action potentials and potassium permeability activation in pancreatic B-cells. *American Journal of Physiology.* 239:C124–C133.

Ribalet, B., and P. M. Beigelman. 1982. Effects of sodium on B-cell electrical activity. *American Journal of Physiology.* 242:C296–C303.

Rorsman, P., P. Arkhammar, and P. Berggren. 1986. Voltage-activated Na^+ currents and their suppression by phorbol ester in clonal insulin-producing RINm5F cells. *American Journal of Physiology.* 251:C912–C919.

Rorsman, P., and G. Trube. 1986. Calcium and delayed potassium currents in mouse pancreatic B-cells under voltage-clamp conditions. *Journal of Physiology.* 374:531–550.

Salomon, D., and P. Meda. 1986. Heterogeneity and contact-dependent regulation of hormone secretion by individual B cells. *Experimental Cell Research.* 162:507–520.

Satin, L. S., and D. L. Cook. 1985. Voltage-gated Ca^{2+} current in pancreatic B-cells. *Pflügers Archiv.* 404:385–387.

Smith, P. F., E. H. Luque, and J. D. Neill. 1986. Detection and measurement of secretion from individual neuroendocrine cells using a reverse hemolytic plaque assay. *Methods in Enzymology.* 124:443–465.

Sturek, M., and K. Hermsmeyer. 1985. Two different types of calcium channels in spontaneously contracting vascular smooth muscle cells. *Journal of General Physiology.* 86:23*a*. (Abstr.)